

A1337/A1338 System Timing

By Bill Wilkinson, Allegro MicroSystems

Introduction

This application note provides a brief description of the internal signal processing delays of the A1337 and A1338 angle sensors. To understand the different sources of delay within both the analog and digital domains, a basic understanding of the front-end transducer is needed. This note starts with a high-level overview of the Circular Vertical Hall (CVH) technology used within the A1337/A1338. Following this, the sources and amount of signal delay are analyzed, using at first a simplistic stationary angle case and then a more complicated rotational example.

The A1337 and A1338 are high-speed high-accuracy magnetic angle sensor ICs, ideal for motor position sensing. Due to the need for precise commutation of modern-day brushless DC (BLDC) motors, the latency inherent with sensing and reporting shaft location can have appreciable impact on performance. Many times, this latency is compensated for on a system level via the microcontroller. This note will examine the typical latency encountered with A1337/A1338 angle sensor ICs.

CVH Basics

The CVH consist of an n-well ring with a series of equally spaced contacts. This geometry allows the detection of a two-dimensional magnetic vector in the same plane as the silicon, as shown in Figure 1.

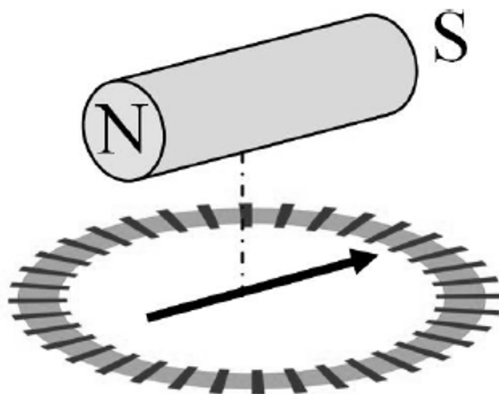


Figure 1: Circular Vertical Hall with a Permanent Magnet Above [1]

When in operation, five contacts are connected together to form the equivalent of one vertical Hall plate. By switch-

ing in contacts, the active segment can be made to “slide” around the entirety of the ring. As the transducer “slides” through a complete 360° rotation, a stepped sine wave is produced as the output of the CVH front-end circuit.

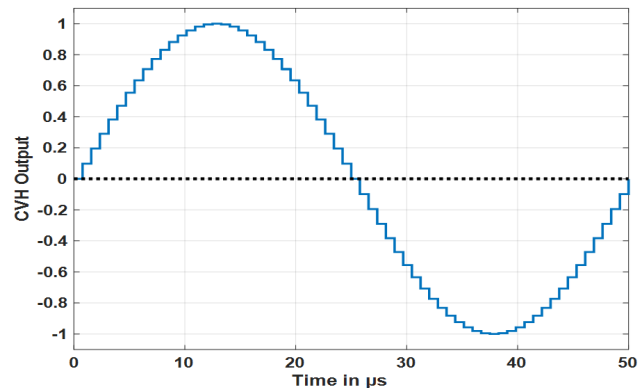


Figure 2: Theoretical CVH Output for a Stationary or Rotating Magnet

It is important to note that this sine wave is a function of the electrical switching around the CVH, not the rotation of the magnetic field. As long as the electrical rotation is significantly greater than the magnetic rotation (10 to 100×), it can be assumed that the sine wave is similar for both a stationary and a rotating magnetic field.

The A1337 and A1338 feature a CVH cycle time (t_{CVH}) of 50 μ s. Every t_{CVH} , the sensor completes a full 360° rotation around the CVH ring. This is equivalent to a rotation rate of 1.2 million RPM, orders of magnitude faster than the fastest expected magnet rotation.

MEASURING ANGLE

As the magnetic field is rotated, the resulting sine wave from the CVH is shifted along the x-axis—in other words, a positional change in the magnetic field is represented as a phase change in the sinusoidal output of the CVH. This is represented in Figure 3 and Figure 4. If the magnetic field is moved by an angle α , the phase of the sinusoid from the CVH will shift by a proportional amount. In fact, because the period of a sine wave is 360°, the phase shift in degrees will ideally match the angle change, α , in degrees.

To determine the phase shift in the sinusoidal signal, the location of the zero-crossing is used and compared against

a reference location (the default 0° location). As the sine wave is shifted left or right, the zero-crossing location will move, indicating the amount of phase shift and thus the amount of angular rotation. By only looking at the zero-crossing point, angle accuracy is relatively immune to changes in sine wave amplitude, which is proportional to magnetic field strength. This allows operation with a wide range of field intensities, up to and beyond 1000 G.

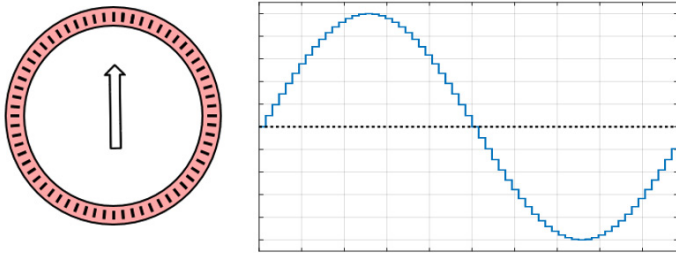


Figure 3: Magnetic Vector Relative to CVH (left) and CVH Output (right)

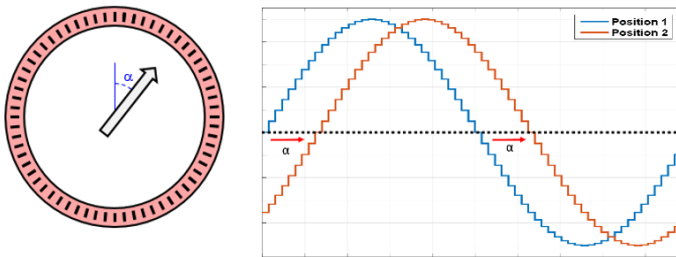


Figure 4: New Magnetic Position (left) and CVH Output Corresponding to New Angular Position (right)

A1337 AND A1338 SIGNAL PATH

A high-level block diagram of the A1337 and A1338 signal path is shown below in Figure 5. The purpose and characteristic timings associated with each block will be discussed individually.

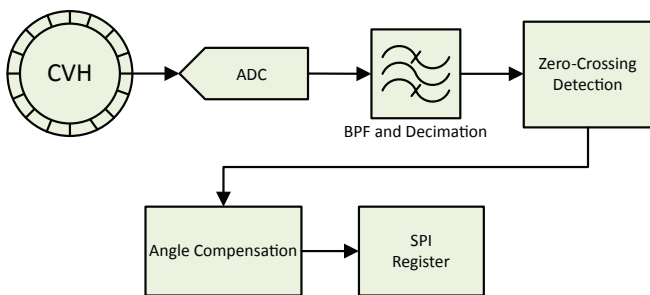


Figure 5: Typical Signal Path Block Diagram

CVH

As described above, the CVH is the front-end transducer of the A1337/A1338. A full electrical rotation of CVH is completed

every t_{CVH} (50 μ s), resulting in a sinusoidal output signal. The phase of the sine wave is used to measure the two-dimensional angle of the magnetic field.

SIGNAL CONVERSION, FILTERING AND DECIMATION

Conversion to the digital domain is accomplished via a high-speed high-resolution ADC. Following this, the signal is filtered via a bandpass filter to remove noise originating from the analog front end. The output is then decimated down to 16 sample points per t_{CVH} for further processing.

The time require for analog-to-digital conversion as well as signal filtering and decimation is typically 40 μ s (t_{FILTER}), with the BPF responsible for the majority of the delay time.

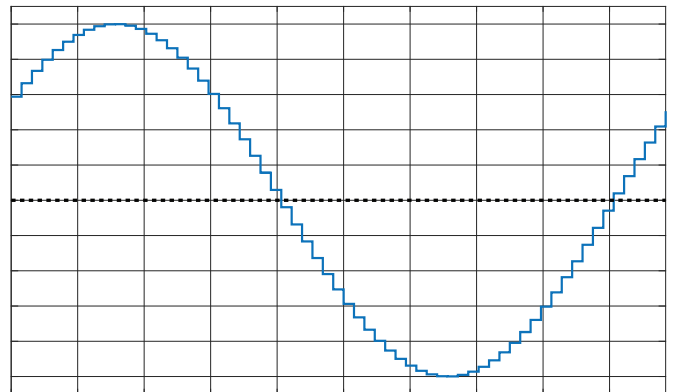


Figure 6: Ideal CVH Output over 1 t_{CVH}

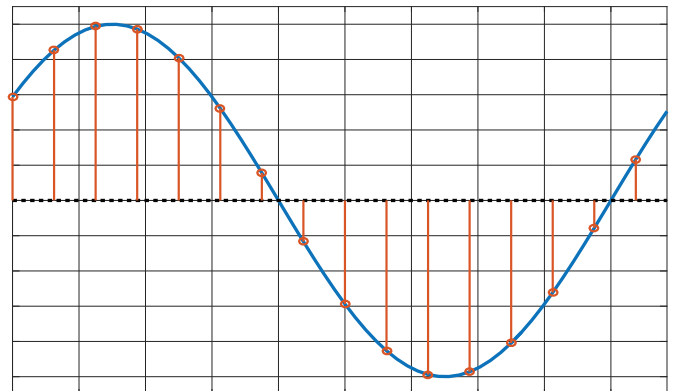


Figure 7: Corresponding BPF Output. Sampled at 16 points. Output will be delayed by t_{FILTER} (40 μ s).

ZERO-CROSSING DETECTION

The zero-crossing of the filtered and decimated sine wave is used to determine the absolute angle position of the magnetic target. The zero-crossing location is determined by a simple signed comparison of the BPF outputs. The detector finds two successive samples where the BPF output transitions from a negative to a positive, or positive to a negative, indicating a crossing of the zero point. This is shown graphically in Figure 8.

Now, because the magnetic angle is stationary in this example, the newly loaded angle in the SPI register will be the same as the value it replaced. Nonetheless, the delays encountered in the static case can be applied to the slightly more complicated “dynamic case” in which the magnet will be rotating, and thus each successive angle reading will produce a different value.

Signal Delay with a Rotating Target (Ideal Case)

When analyzing the sensor response time for a changing magnetic angle value, the two main sources of signal delay discussed in the preceding section are still applicable: the filter delay and the compensation delay. In addition to the intrinsic processing delays of the sensor, an external source of delay must now be considered—when the SPI register is polled by the host controller.

Figure 11 provides a graphical representation of the delay time encountered for a dynamically changing angle value. For simplicity, the internal signal from the CVH is not shown, and instead the delays are represented by horizontal lines, the length of which are proportional to the magnitude. The magnetic angle value is shown linearly increasing over time (thus at a fixed RPM), with dashed vertical lines indicating zero-crossing of the CVH sine wave, similar to Figure 10. These are assumed to occur every t_{update} , or 25 μs ; some deviation does occur, and will be discussed later for the non-ideal case.

Working backwards through Figure 11, the SPI register is sampled by the host microcontroller at time t_s , indicated by the green arrow. Since the angle value within the register was loaded sometime prior to t_s , this time will be denoted as t_{Async} , as the sensor and SPI bus operate asynchronously to one another. Prior to loading the angle into the SPI register, the value is compensated for temperature and intrinsic errors and filtered, incurring the delays t_{comp} and t_{FILTER} . Thus the total delay time from when the CVH front end “sees” a zero-crossing (M0) and the corresponding angle data (D0) is read is:

$$t_{delay(dynamic)} = t_{FILTER} + t_{comp} + t_{Async} \quad (2)$$

As with the static case, the SPI register is updated every t_{update} period, or 25 μs , and is 46 μs old at this point. The additional term present, t_{Async} , is dependent on when the host samples the angle value relative to the updated time of the SPI register. If the host samples the register immediately after the new value is loaded (far left side of the D0 block in Figure 11), t_{Async} is zero, with no additional delay incurred. However, it is also possible for the host to initiate an SPI transaction just prior to the next angle value being loaded (right side of the D0 block), in this case t_{Async} is equal to the update period, t_{update} . Thus t_{Async} can vary between 0 and t_{update} .

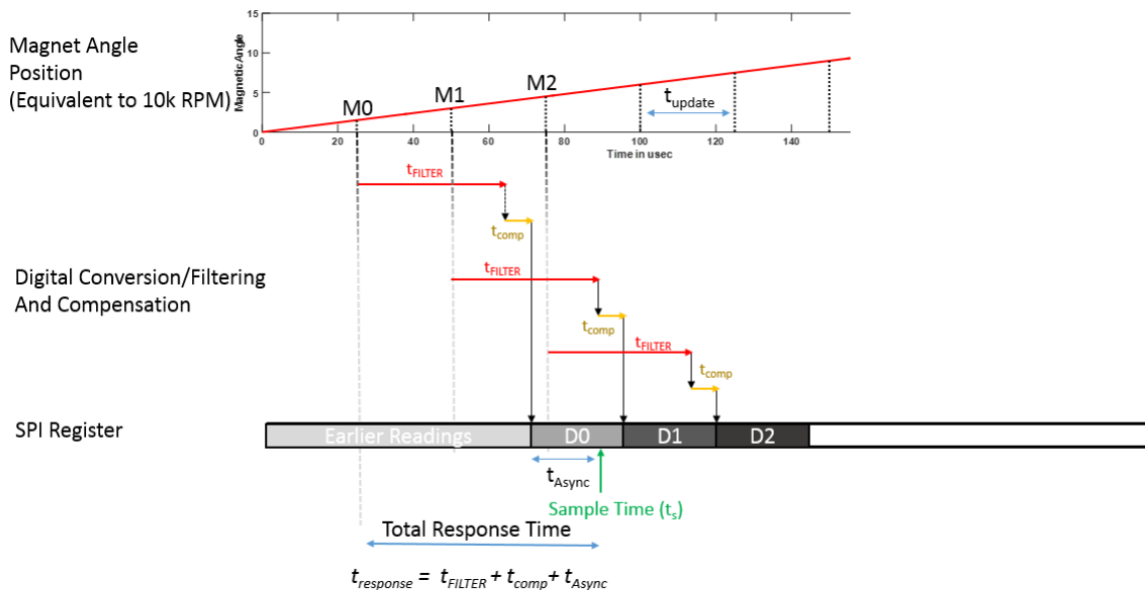


Figure 11: Signal Propagation Delays, Dynamic Case

Thus the total age of the angle value can vary between:

$$\text{Minimum } t_{\text{Delay}(\text{ideal})} = 40 \mu\text{s} + 6 \mu\text{s} + 0\mu\text{s} = 46\mu\text{s}$$

and

$$\text{Maximum } t_{\text{Delay}(\text{ideal})} = 40 \mu\text{s} + 6 \mu\text{s} + 25 \mu\text{s} = 71 \mu\text{s}$$

These two values represent the possible extremes; in practice, the measured response time will approach the average of the two values, $\approx 60 \mu\text{s}$.

TIME VARIATIONS IN ZERO-CROSSING COUNTERS

In the preceding description, the period between zero-crossing detection events—and thus the angle update rate—was assumed to be $25 \mu\text{s}$. While this is the case for a perfectly stationary position, as the magnetic vector rotates the update period will deviate slightly.

As shown in Figure 8, the output of the CVH is digitally sampled 16 times for every CVH cycle (t_{CVH}), which is completed every $50 \mu\text{s}$. Thus, a new sample occurs every $3.125 \mu\text{s}$. A zero-crossing is determined by detecting a change in sign across two successive samples. For the sine-wave depicted in Figure 12, corresponding to an arbitrary “Angle Position One”, the first zero-crossing is detected at sample point S[7]. The second is detected at S[15]. These two points are 8 samples apart, thus separated in time by $25 \mu\text{s}$. This update period will maintain for as long as the sine wave zero-crossing occurs within those same two sections (i.e. between S[6] and S[7] and between S[14] and S[15]).

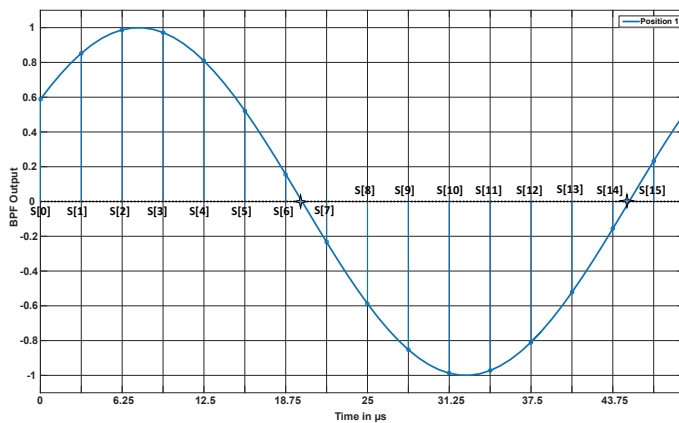


Figure 12: Zero Crossing Locations, Magnet Position One

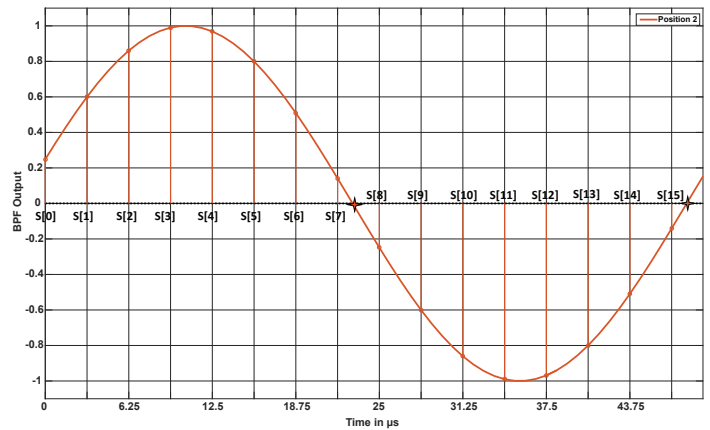


Figure 13: Zero Crossing Locations, Magnet Position Two

However, as the magnetic vector rotates, the sine wave is shifted in phase, moving the zero-crossing point. For example, if it is assumed on the next CVH cycle the magnetic vector was changed from “Position One” to “Position Two”, resulting in the sine wave depicted in Figure 14, the zero-crossing location is shifted to the right. It will now be detected one sample later, at S[8]. This is a total of 9 sample periods from the previous zero-crossing detection (S[15] from Position One), corresponding to $28.125 \mu\text{s}$. Provided the magnetic vector does not cross another sample boundary, the following zero-crossing will be detected at S[0] on the next CVH cycle—8 sample points later—restoring the $25 \mu\text{s}$ update period. Thus the angle update rate will vary by $3.125 \mu\text{s}$ when the zero-crossing location moves across sample boundaries. Each boundary is equivalent to 16th of a full rotation, or 22.5° .

Another way to visualize this phenomena is to view the 16 sample points as equally distributed around a unit circle (representing the CVH). The sample points trace out 16 sections, like slices of a pie. The zero-crossing of the sine wave generated from the CVH will occur at the intersection of the magnetic vector and the circle. Initially, these intersections occur in the sections between S[6] and S[7], as well as S[14] and S[15], resulting in the zero-crossing detection points shown in Figure 14. Eventually, as the magnetic vector rotates, it will transition from one section to the next adjacent section (for example, moving from the section circumscribed by S[6]/S[7] to the S[7]/S[8] section). It is during this transition that an additional sample point is required to detect the zero-crossing.

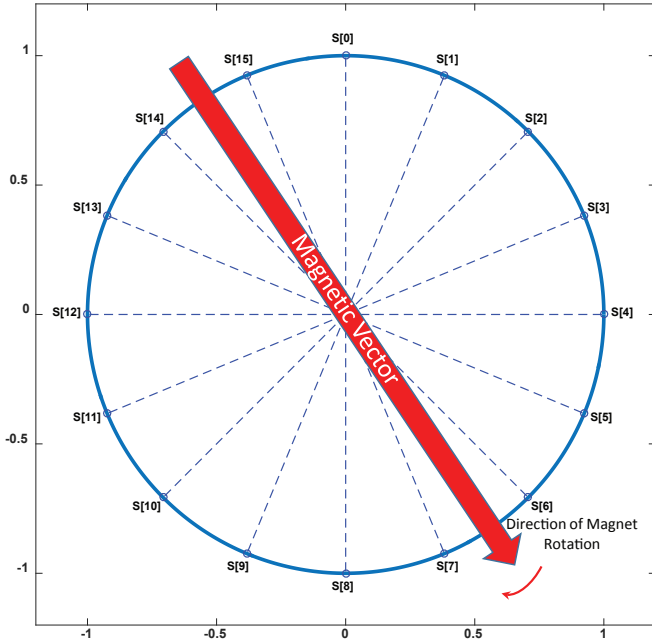


Figure 14: Geometric Representation of CVH Sampling

Each of the 16 sections created by the sampling of the CVH output represents 22.5° of a full rotation. At ten thousand RPM, 375 μs are required for a magnet to traverse 22.5°. In this time, the CVH will have completed 7.5 cycles. Because of this high CVH cycle rate, it is not possible for a magnetic vector to transition by more than one section within a single update period. This restricts the variability of the angle update rate to 3.125 μs.

Because this transition from one section to another is dependent on rotation direction, the 3.125 μs variance can either add to or subtract from the nominal 25 μs update period.

When analyzing the response time for the “Rotating Angle Case”, the total delay time was defined as:

$$t_{delay(dynamic)} = t_{FILTER} + t_{comp} + t_{Async}$$

where t_{Async} could vary from 0 to t_{update} , and t_{update} described the angle update period. Initially, this value was assumed to be 25 μs. After taking into account the section transitions of the CVH, t_{update} is now:

$$t_{update} = 25 \mu s \pm 3.125 \mu s$$

Taking these factors into account, the final response time is:

$$Minimum t_{Delay} = 40 \mu s + 6 \mu s + 0 \mu s = 46 \mu s$$

$$Maximum t_{Delay} = 40 \mu s + 6 \mu s + 28 \mu s = 74 \mu s$$

Conclusion

The CVH provides several advantages when compared to other methods of angle detection; it is fast, not susceptible to channel offset, and relatively independent of field strength variations. These advantages are tied to the unique way in which the angle information is detected and processed. These same unique attributes result in an added layer of complexity when attempting to analyze and determine system response time. Despite these apparent difficulties, with a basic understanding of the transducer and processing chain, the maximum and minimum expected signal delays can be determined.

$$Minimum t_{Delay} = 46 \mu s$$

$$Maximum t_{Delay} = 74 \mu s$$

In practice, these extremes occur rarely. When averaged over multiple angle samples, the measured delay will approach the mean value of:

$$Mean t_{Delay} = 60 \mu s$$

References

- [1] P. Kejik, S. Reymond, R.S. Popovic, “Circular Hall Transducer for Angular Position Sensing”, Transucers & Eurosensors '07, Lyon, France, June 2007. Pp 2593-2596.

Revision History

Number	Date	Description
-	November 14, 2019	Initial release

Copyright 2019, Allegro MicroSystems.

The information contained in this document does not constitute any representation, warranty, assurance, guaranty, or inducement by Allegro to the customer with respect to the subject matter of this document. The information being provided does not guarantee that a process based on this information will be reliable, or that Allegro has explored all of the possible failure modes. It is the customer's responsibility to do sufficient qualification testing of the final product to ensure that it is reliable and meets all design requirements.

For the latest version of this document, visit our website:

www.allegromicro.com